Deep Learning and Power Allocation Analysis in NOMA System

Mohamed Gaballa
Electronic & Electrical Engineering
Brunel University London
Uxbridge, UK
mohamedgaballa.gaballa@brunel.ac.uk

Maysam Abbod
Electronic & Electrical Engineering
Brunel University London
Uxbridge, UK
maysam.abbod@brunel.ac.uk

Ammar Aldallal
Telecommunication Engineering
Ahlia University
Manama, Bahrain
aaldallal@ahlia.edu.bh

***Abstract*— This study shows how the channel estimation based Deep Learning (DL) and a power allocation method are together employed for multi-user detection in a Power domain Non-Orthogonal Multiple Access (PD-NOMA) network. Successive interference cancellation (SIC) procedure is typically employed at receiver side, where numerous users are decoded in a successive approach. Fading channels may scatter transferred signal and initiate dependencies between scattered components, this might influence the channel estimation technique and therefore impact the SIC procedure and signal recognition precision. In our proposed scheme, the influence of Deep Neural Network (DNN) in clearly approximating the channel parameters for users in NOMA cell is inspected. In our scenario, we incorporate the Long Short Term Memory (LSTM) layer with NOMA cell where the LSTM is employed for complex data management to perform training and predication. The DNN is trained online on basis of random channel models and then the trained network is used to approximate the channel taps that will be utilized by the receiver in recovering the desired symbols. Additionally, power factors for user's devices are optimized to maximize the sum-rate of users where whole power and Quality of service (QoS) restrictions are considered. Simulation outcomes in terms of Bit Error Rate (BER), Outage probability, and sum rate have shown the dominance of the suggested channel estimation using DL over standard estimation approach. Moreover, both fixed power and optimized power schemes are also assessed when DNN is applied.**

Keywords—DL, LSTM, DNN, NOMA, SIC

I. Introduction

Non-orthogonal multiple access (NOMA) system is categorized as an encouraging multiple access technique in forthcoming wireless systems toward improving spectral efficacy and system throughput. NOMA system can develop the current resources essentially by opportunistically getting benefit of the users' channel environments then deliver diverse quality of service (QoS) requirements for current users in the system. NOMA enables various users to get concurrent access to same time-frequency resources by principle of superposition different signals in the power or code ranges [1]. The idea of NOMA is based on that, user with bad channel surroundings could be shared with user with good channel status on same assigned subcarrier at same time slot, in order that the spectrum can be effectively exploited. In NOMA system, each user equipment can receive the superposition of signals from users in the cell, hence the exclusion of interference from non desired users come to be essential for managed decoding. Commonly, multi-user recognition in NOMA can be achieved via SIC scheme that can be performed in power domain. In SIC procedure, signals from different users are decoded sequentially on the basis of the assigned power beside channel state information (CSI). Broad knowledge of CSI for each user is demanding because pilot symbols employed in channel prediction might interfere with signals from another users, hence affecting the effectiveness of conventional channel approximation methods, such as minimum mean square error (MMSE) [2].

Deep learning (DL) procedures have the potential to adjust to alterations in the path among user and base station (BS) and can approximate the channel coefficients for each device, therefore DL is regarded as reliable contenders for upcoming wireless systems.

In [3], the authors introduced a channel estimation procedure for multi-user detection scheme with imperfect CSI. Discrete state model and Kalman filter are employed to make an estimate of the unspecified parameters of a varying channel based on uncertainty pattern. Authors inspected the censoring phenomenon via the Tobit measurement scheme to accomplish further precise estimation, while the QoS demands such as minimum signal to interference and noise ratio (SINR) are satisfied for all users. Also, a robust mean square error (MSE) estimation framework is created to minimize the estimation error. Analytical analysis, and simulation outcomes validated the efficiency of the framework in terms of channel estimation reliability.

Authors in [4], investigated changes in the throughput and outage probability versus signal to noise ratio (SNR) in NOMA network, on the basis of two categories of partial channel state information. Authors have discussed both imperfect CSI and second order statistics (SOS) based NOMA and proved that SOS scheme can realize improved performance than the performance attained with imperfect CSI, but it may reach comparable performance to NOMA with ideal CSI at low SNR. Results also revealed that NOMA system can attain improved performance compared to conventional orthogonal multiple access (OMA) approach when partial channel state information is applied.

In [5], a pilot-assisted receiver framework is proposed for uplink SIMO-NOMA system, that incorporates a mixed channel approximation and signal recognition framework. Authors gather DL algorithm with SIC identification scheme to diminish the factors need to be learned.

Moreover, signal recognition precision enhancement and noise alleviation have been accomplished by introducing interference and noise removal parameters at SIC phase. Simulation outcomes show that the BER performance in terms of the suggested deep learning structure is better than conventional MMSE method and the complication of receiver is reduced.

In [6], authors have introduced a semi-blind recognition method based on DL, to detect signals for users in co-operative NOMA network. With the aid of DL scheme and pilot symbols responses, the suggested approach is able to detect signals while no separate channel estimation process is required. The DL network trained offline over Rayleigh fading environment and then the trained model is utilized as online detector. Authors also, examined the trained model using Rician and Nakagami fading models and simulation consequences prove that the proposed deep learning detector outperforms traditional detectors.

II. System Model

In this section, downlink NOMA system is analyzed where users are connected to BS via numerous channel gains. In our NOMA cell, it is assumed that we have one BS with one antenna to assist two users simultaneously and every user's device also holds one antenna. Naturally, in NOMA cell users are receiving the superimposed signal sent from BS that include desired and interfering signals, sent via same resource block. Accordingly, incorporating a mixture of signals using diverse power levels is crucial to strengthen SIC technique [7] and assist in differentiating between signals at each receiver equipment.

In PD-NOMA, users that distinguished by good or strong channel conditions are frequently assigned minimum power, while users with weak path circumstances can be assigned more power factors. Each user is labelled by its fading channel and the distance from BS. In our system we can identify the nearby equipment as near user and equipment at edge of cell is known as far user. In the examined cell, a Rayleigh fading channel is assumed for the links among BS and each user. On the basis that there are two users in the examined cell, the fading path for each user can mathematically be specified with the following, for near device $h_n \sim (0, d_n^{-k})$ and for far device $h_f \sim (0, d_f^{-k})$, where h_i represent the fading path connecting user equipment and BS, and k denotes path loss exponent [10].

In this paper, noise samples are considered as Additive White Gaussian Noise (AWGN), with zero mean and noise power indicated as σ^2. With no lack of generality, we can consider that $|h_n|^2 > |h_f|^2$. Total transferred power from BS to users in the cell is identified by P_t. In NOMA cell, the receiver at each equipment has the capability to perform SIC to remove signals related to users with weak link conditions. Alternatively, signals belong to users with good channel circumstances treated as interference. At BS, the antenna knows how to send the superposition coded signal x which is formulated as follows [8]

$$x = \sqrt{P_t}\left(\sqrt{\alpha_n}x_n + \sqrt{\alpha_f}x_f\right) \qquad (1)$$

Where α_n, and α_f are the power factors for near and far users independently. Similarly, x_n, and x_f represent the required signals related to near, and far users separately. Therefore, received signal at far user can be stated as follows [8]

$$y_f = xh_f + z_f \qquad (2)$$

Where h_f denotes the fading path between BS and far user, while z_f denotes AWGN noise part at far device with zero mean and σ^2 variance. Far user is typically depicted by weak path environment, thus the signal x_f can be given more power by BS where $\alpha_f > \alpha_n$. Thus, the receiver equipment for far user will be able to straightway interpret his own message x_f from y_f. Signal obtained at far user can mathematically expanded as follows:

$$y_f = \sqrt{P_t\alpha_f}x_f h_f + \sqrt{P_t\alpha_n}x_n h_f + z_f \qquad (3)$$

The 1st term in (3) indicates the far user's desired signal, and the 2nd term denotes the interference signal. Based on (3) The far user rate could be formulated as

$$R_f = \log_2\left(1 + \frac{|h_f|^2 P_t\alpha_f}{|h_f|^2 P_t\alpha_n + \sigma^2}\right) \qquad (4)$$

Typically, near user is characterized by good channel condition, so the signal received at near user equipment is simply formulated as follows:

$$y_n = xh_n + z_n$$
$$y_n = \sqrt{P_t\alpha_n}x_n h_n + \sqrt{P_t\alpha_f}x_f h_n + z_n \qquad (5)$$

The 1st term in (5) characterizes the expected signal for near user, and the 2nd component in (5) is the interfering far user term. In addition, it is noted from (5), that the 2nd term is prevailing due to further power designated to far user. Thus, at receiver of near user, immediate decoding for far user signal x_f should be accomplished at first. After SIC, the achieved rate for near user R_n to decode its own required signal x_n can be expressed as

$$R_n = \log_2\left(1 + \frac{|h_n|^2 P_t\alpha_n}{\sigma^2}\right) \qquad (6)$$

III. Power Allocation

The purpose is to maximize the sum-rate for active users in examined cell based on optimizing power coefficients for users in compliance with applied channel gains. The summation of aforementioned sum-rates for N-users downlink NOMA cell can be formulated as shown

$$R_{sum} = \sum_{k=1}^{N} \log_2\left(1 + \frac{|h_k|^2 P_t\alpha_k}{|h_k|^2 \sum_{j=1}^{k-1} P_t\alpha_j + \sigma^2}\right) \qquad (7)$$

1. Total Power constraint

Designated power for each device in examined cell is a fraction of the whole power P_t conveyed by BS. Therefore, power portion given for each device need to follow [9]

$$\sum_{x=1}^{N} \alpha_x \leq 1 \qquad (8)$$

where α_x is the power fraction for x^{th} user.

2. QoS constraint

To develop user fairness, we can assume that user with bad channel environment in NOMA cell has a QoS demand, which indicates that a lowest possible rate R_{min} needs to be assured and consistent with the examined optimization problem, this constraint can be formulated as shown [9]

$$\log_2(1+\delta_n) \geq R_{min} \tag{9}$$

Based on the above-mentioned constraints in (8) & (9) and sum rate representation, the typical optimization problem can be shown in this way [8][9]:

$$\max_{\alpha} R_{sum} = \sum_{k=1}^{N} \log_2\left(\frac{|h_k|^2 P_t \sum_{j=1}^{k-1}\alpha_j + \sigma^2 + |h_k|^2 P_t \alpha_k}{|h_k|^2 P_t \sum_{j=1}^{k-1}\alpha_j + \sigma^2}\right) \tag{10}$$

such that

$$\sum_{x=1}^{N} \alpha_x \leq 1$$
$$\log_2(1+\delta_n) \geq R_{min}$$
$$\alpha_k \geq 0 \;\; \forall k = 1,2,\ldots,N$$

IV. Optimization Investigation

Power optimization in this section is accomplished with respect to two users in NOMA cell and the optimization problem can easily redeveloped as shown

$$\max_{\alpha} \quad R_{Sum} = R_n + R_f \tag{11}$$

$S.t.$

$$(2^{R_{min}}-1) - |h_k|^2\rho\left(\alpha_m - (2^{R_{min}}-1)\sum_{i=1}^{m-1}\alpha_i\right) \leq 0$$
$$\alpha_n + \alpha_f - 1 \leq 0$$
$$\alpha_n\,,\ \alpha_f \geq 0$$

Where $m = 2$ and R_{min} is the minimum rate needed in the cell. In accordance with the aforementioned analysis, the constraints can be expressed as shown:

$$C_1(\alpha) = \alpha_n + \alpha_m + \alpha_f - 1 \tag{12}$$
$$C_2(\alpha) = (2^{R_{min}}-1) - \rho|h_m|^2(\alpha_m - (2^{R_{min}}-1)(\alpha_n) \tag{13}$$

The constraints $C_1(\alpha), C_2(\alpha)$ are linear in terms of α , then $C_1(\alpha), C_2(\alpha)$ are convex. Now we need to calculate $\nabla R_{Sum}(\alpha)$ & $\nabla^2 R_{Sum}(\alpha)$. Firstly, we can derive a general expression for the first derivative for $R_{Sum}(\alpha)$ in terms of the power factor α_i . After certain mathematical manipulations, $\nabla R_{Sum}(\alpha)$ can generally be represented as follows [8]

$$\frac{\partial R_{Sum}}{\partial \alpha_i} = \frac{1}{ln2}\left(\frac{|h_i|^2 P_t}{|h_i|^2 P_t \sum_{j=1}^{i}\alpha_j + \sigma^2}\right) - \frac{1}{ln2}\sum_{k=1}^{N-i}\left\{\left(\frac{\left(\left|h_{(i+k)}\right|^2 P_t\right)^2 \alpha_{i+k}}{\left(\left|h_{(i+k)}\right|^2 P_t \sum_{j=1}^{i+k}\alpha_j + \sigma^2\right)}\right) \times \left(\frac{1}{\left(\left|h_{(i+k)}\right|^2 P_t \sum_{j=1}^{i+k-1}\alpha_j + \sigma^2\right)}\right)\right\} \tag{14}$$

Similarly, we can deduce a general expression for the second derivative for objective function $R_{Sum}(\alpha)$ with respect to power coefficient α_i . The general derived form can be formulated as follows:

$$\frac{\partial^2 R_{Sum}}{\partial {\alpha_i}^2} = -\frac{1}{ln2}\left\{\left(\frac{(|h_i|^2 P_t)^2}{\left(|h_i|^2 P_t \sum_{j=1}^{i}\alpha_j + \sigma^2\right)^2}\right) - \sum_{k=1}^{N-i}\left\{\left(\frac{\left(\left|h_{(i+k)}\right|^2 P_t\right)^3 \alpha_{i+k}\left[2\left(\left|h_{(i+k)}\right|^2 P_t \sum_{j=1}^{k+i-1}\alpha_j + \sigma^2\right) + \left|h_{(i+k)}\right|^2 P_t \alpha_{i+k}\right]}{\left(\left|h_{(i+k)}\right|^2 P_t \sum_{j=1}^{i+k}\alpha_j + \sigma^2\right)^2}\right) \times \left(\frac{1}{\left(\left|h_{(i+k)}\right|^2 P_t \sum_{j=1}^{i+k-1}\alpha_j + \sigma^2\right)^2}\right)\right\}\right\} \tag{15}$$

Rather than utilizing a Hessian matrix to demonstrate that the objective function is concave, we can make use of the following conditions [8][9]

1. $\frac{\partial^2 R_{Sum}}{\partial \alpha_n^2} < 0$ (16)
2. $\frac{\partial^2 R_{Sum}}{\partial \alpha_f^2} < 0$ (17)
3. $\left(\frac{\partial^2 R_{Sum}}{\partial \alpha_f^2}\frac{\partial^2 R_{Sum}}{\partial \alpha_n^2} - \left(\frac{\partial^2 R_{Sum}}{\partial \alpha_n \partial \alpha_f}\right)^2\right) > 0$ (18)

Conditions (16) (17) (18) have been satisfied which implies that the objective function is concave and has a distinctive global upper limit. Lagrange function and the KKT conditions can be applied to obtain optimum power parameters. After some mathematical replacements, the analytical form expression for the power factors can be formulated as shown [10]

$$\alpha_n = \frac{1}{\left(2^{R_f}\right)}\left(\frac{\rho|\mathrm{h}_n|^2 - (2^{R_f}-1)}{\rho|\mathrm{h}_n|^2}\right) \tag{19}$$
$$\alpha_f = \frac{(2^{R_f}-1)}{(2^{R_f})}\left(\frac{\rho\left|h_f\right|^2 + 1)}{\rho\left|h_f\right|^2}\right) \tag{20}$$

V. RNNs and LSTM

Recurrent Neural Networks (RNNs) are considered as a set of controlled learning procedure, where RNNs can manage consecutive data sequences for estimation and identification [11].

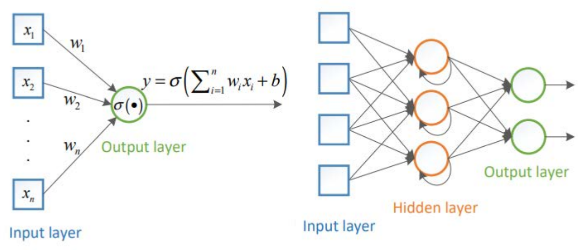

(a) Single neuron element. (b) Recurrent neural network (RNN).

Fig. 1 RNN network construction [11]

As shown in Fig. 1, in RNNs hidden layers have the potential to play a role as buffer for the network at a certain time, this arrangement allows the RNNs to deal with prior complex data for an extended interval of time. In addition, RNNs can characterize time dependencies between data sequences with a smaller number of neurons. Alternatively, conventional RNN based on backpropagation encounters vanishing gradient problem and slow-going in learning process [2][11]. Thus, RNNs will not be the most appropriate neural network for signals that send out over fading links which may diffuse the signal and initiate a long term dependencies among its components [12]. LSTM, which is a one type of RNNs, is frequently employed for classification based on time series data, where it can recognize the time dependencies among data sequences [12]. LSTM layer include LSTM cells, and every cell comprises a collection of gates as shown in Fig. 2. Based on the underlying design, the LSTM gates are capable to save and gain access to data for long intervals of time and also counteract the error raised by backpropagation method [2][12]. LSTM has the capability to deal with vector of complex data, thus incorporating the amplitude and phase components of input sequence simultaneously. LSTM is appropriate choice to deal with multi-user recognition when time series data is presented [13].

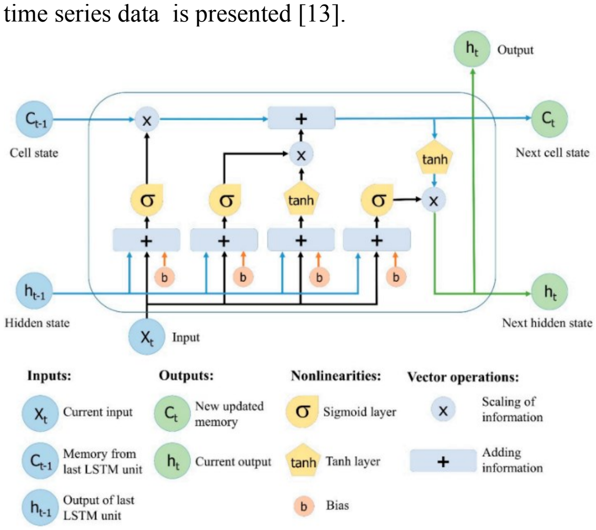

Fig. 2 Internal structure of LSTM cell

VI. LSTM AND NOMA STRUCTURE

A framework that incorporate the LSTM network with NOMA system is introduced here. In data driven communication, the quantity of LSTM cells at every single layer and the amount of LSTM layers can be implemented through empirical observations, to make sure that adding up additional LSTM layers will not produce an obvious gain in learning stage or remarkably influence the network convergence [14]. In our DL scheme, the LSTM network involves 4 layers, each layer is supported by a number of neurons, and weighted sum of these neurons are going to enter to a nonlinear activation function. In proposed LSTM configuration, the input layer consists of 128 neurons, and the vector of data feeded to input layer are transferred to the following layer with the aid of weight coefficients, bias, and activation function. In the next layer, we apply single LSTM layer with 200 hidden elements. The adjustable weights of LSTM layer are recurrent $\boldsymbol{R}$, input $\boldsymbol{W}$, and bias $\boldsymbol{b}$. The 3rd layer in our DNN model is a fully-connected (FC) layer which handles the outcomes of LSTM layer. The end layer is regression layer that is responsible for updating network weights and biases in addition to update the state of the cell.

In LSTM cell, the output is produced on the basis of the recent input and the prior cell state. LSTM cell contains a various kinds of gates, forget, input , and output gates. These gates will aid in remembering the preceding cell state and decide if the previous state need to be employed or not when calculating the output. In addition, LSTM is characterized by two main states, the cell state C_{t-1} which is known as inner buffer where all responses are accumulated, and the other state is called hidden state h_{t-1} that are exploited for calculating the output. Fig. 2 shows the inner configuration of LSTM cell, where t indicate the time instant, x_t is the recent input, h_{ti} denote the recent output channel parameters for user i at time t, and C_{t-1} is the former cell state [14].

VII. DEEP LEARNING SYSTEM ARCHITECTURE

The transmitted frame is consisting of data and pilot symbols. The fading path is considered as constant spanning over one frame and the fading path change from one frame to another. In our algorithm, to implement an efficient Deep Neural Network (DNN) model for channel approximation, two phases are included. In the first phase, online training is conducted, where the DNN layers are mainly trained with a diverse Rayleigh channel coefficients [11][14]. In implementation phase, the trained DNN model will be employed to generate the estimated fading coefficients explicitly for users, then the estimated coefficients will be utilized to retrieve the desired original signals. The proposed DL algorithm for channel approximation can be listed as indicated in algorithm 1.

Algorithm 1: Channel Estimation based DL scheme

1. Initialize adjustable parameters of an LSTM layer ($\boldsymbol{W}, \boldsymbol{R}, \boldsymbol{b}$), the input $\boldsymbol{W}$, the recurrent $\boldsymbol{R}$, and bias $\boldsymbol{b}$.
2. Produce random Rayleigh channel parameters for users
3. Create known-pilot symbols
4. Characterize the training & testing sequences $(\boldsymbol{Z_T}, \boldsymbol{Z_S})$
5. Define Length of training and testing sequences $(\boldsymbol{L_S}, \boldsymbol{L_T})$
6. Set the power coefficients for users initially.
7. Compute the mean and variance of training data $(\boldsymbol{\mu_T}, \boldsymbol{\sigma_T^2})$
8. Normalizing the training data $\boldsymbol{Z_T} \rightarrow \boldsymbol{Z_{NT}}$
9. Characterize the relationship between Consecutive normalizing training sequences $(\boldsymbol{X_{NT}}, \boldsymbol{Y_{NT}})$
10. Initialize the training network $(\boldsymbol{T_{net}})$
11. Apply $(\boldsymbol{X_{NT}}, \boldsymbol{Y_{NT}})$ as inputs for training model
12. Update training model $(\boldsymbol{T_{net}})$ & Predict output coefficients $(\boldsymbol{Y_{NP}})$
13. for I =1 : $\boldsymbol{L_T}$
    $[\boldsymbol{T_{net}}, \boldsymbol{Y_{NP}}]$ = predictAndUpdateState $(\boldsymbol{X_{NT}}, \boldsymbol{Y_{NT}})$
    end
14. Denormalize $\boldsymbol{Y_{NP}} \rightarrow \boldsymbol{Y_P}$ & calculate RMS $(\boldsymbol{Y_P} - \boldsymbol{Z_S})$
15. Update the state of training network $(\boldsymbol{T_{net}})$
16. using $(\boldsymbol{\mu_T}, \boldsymbol{\sigma_T^2})$, Normalize testing data $\boldsymbol{Z_S} \rightarrow \boldsymbol{Z_{NS}}$
17. Use $(\boldsymbol{Z_{NS}})$ as inputs for trained network $(\boldsymbol{T_{net}})$
18. for I =1:$\boldsymbol{L_S}$
    $[\boldsymbol{T_{net}}, \boldsymbol{Y_{NP}}]$ = predictAndUpdateState $(\boldsymbol{Z_{NS}})$
    end
19. Denormalize $\boldsymbol{Y_{NP}} \rightarrow \boldsymbol{Y_P}$ & calculate RMS $(\boldsymbol{Y_P} - \boldsymbol{Z_S})$

VIII. DL SIMULATION ENVIRONMENT & RESULTS

The simulation settings will be presented in this section. The analyzed downlink NOMA cell includes one BS and two users, where BS and user equipments are all supplied with single antenna. Monte-Carlo simulations are implemented with $N = 10^6$ iterations. At starting of each set of iterations, pilot data are randomly created and identified at BS and at each user equipment. In our simulation scenario, we assume that CSI is not available. Hence, we decide to employ the MMSE classical channel estimation technique scheme [15] in the examined NOMA cell. Power levels are assigned for every user in proportion to his channel gain and current distance from the BS.

Quadrature phase shift keying (QPSK) is employed as modulation method for both data and pilot symbols. modulated signals are multiplexed and sent by BS to all users across uncorrelated Rayleigh fading paths affected by AWGN, and the noise spectral density is $N_0 = -174$ dBm and path loss exponent is 4. At the receiver equipment, the channel estimation procedure will be originated based on LSTM neural network, which employs gradient descent algorithm [14], to enable the LSTM layer to precisely approximate the desired channel coefficients. At starting of each training period, the weights and bias values are prepared at random, while throughout the training period, weights are adjusted in accordance with gradient descent procedure. The performance of the LSTM network is evaluated throughout the training period using root mean square error (RMSE) and loss functions. NOMA factors are assigned based on long term evolution (LTE) standard [16]. Training and testing periods are accomplished online during simulations, and fading parameters produced in testing stage are not the same as in the training phase. After the training and testing periods are ended, the trained model will be working as real-time channel estimator for users. In simulations, the transferred power is mainly varying from 0 to 40 dBm, and in fixed power allocation (FPA) setting, we set $\alpha_f = 0.7$, and $\alpha_n = 0.3$.

In Fig. 3 simulation outcomes show the comparison between channel estimation based DL algorithm and channel estimation based on MMSE for far, and near users in NOMA system in terms of bit error rate (BER) and power transmitted. Both the far and near users show up appropriate enhancement in reducing the BER when DL algorithm is employed compared to MMSE scheme specifically when the applied power is increased. Power saving is approximately 3 dBm for both users, when DL method is applied compared to MMSE method. The dominance of DL effect in lowering the BER compared to MMSE procedure is noticed clearly from simulation outcomes for each user and for different applied power levels.

Fig. 4, illustrates the outage probability metric against power transmitted for the two examined users in NOMA cell when DL and MMSE procedures are applied for channel estimation. Far user simulation outcomes imply an enhancement with 2-3 dB approximately in outage probability when channel approximation based DL is performed compared to MMSE method. Comparably, near user with DL algorithm shows an obvious improvement compared to results achieved by MMSE procedure. It is evident that near user continuously shows good performance compared to far user in terms of both DL algorithm and standard MMSE procedure, this may be explained by the relaxed channel environment for near user.

Simulation outcomes for the sum-rate for users are illustrated in Fig. 5. In this figure, DL algorithm and conventional scheme based on MMSE are also applied for the aim of channel approximation parameters. It is obviously observed that for small SNR, DL channel approximation algorithm shows improvement over the conventional MMSE scenario, and this enhancement increases to more than 1b/s/Hz when transmitted power is also increased. This results proves the success of the DL algorithm in estimating channel parameters prior to signal detection stage.

In Fig. 6 and Fig. 7, two separate simulation environments are implemented to produce this figures. The first simulation scenario when FPA structure is utilized for users in the cell and the other setting when optimized power method is applied and both setups are simulated when DL algorithm is utilized for channel approximation for both users in NOMA cell.

In Fig. 6, for far user case, DL and optimized power scheme simulation outcomes show performance improvement compared to DL with FPA scenario for BER metric vs transmitted power. On the other hand, for near user outcomes, DL based channel approximation together with FPA provide comparable results to optimized power structure, this can be explained that for near user the relaxed channel environments is more effective than distributed power.

In Fig. 7, results for the sum-rate are illustrated, and based on the simulation outcomes, it can be observed that DL and optimized power distribution show slight enhancement in sum-rate compared to DL with FPA method when power applied is low. On the other hand, both optimized power and FPA methods are providing equivalent sum rate when power setting is higher than 15 dBm.

IX. Conclusion

In this work, we introduce and discuss how the channel estimation based LSTM and power optimization are together exploited for multi-user detection in PD-NOMA. In suggested scheme, the influence of DNN in clearly predicting the channel parameters for users in NOMA cell is explored, where LSTM network is employed for complex data management to carry out training, and prediction. The proposed DNN is trained online on the basis of the normalized generated channel parameters. In implementation phase, the trained DNN model will be working to generate the approximated fading parameters, and these predicated channel parameters will be used to retrieve the transmitted data. Simulation results have demonstrated that the implied LSTM assisted NOMA can realize better performance in terms of the BER, Outage probability, and sum rate. Moreover, user's power factors are optimized to maximize the sum rate for users and the performance of the optimized power and fixed power schemes are explored when DL algorithm for channel approximation is applied.

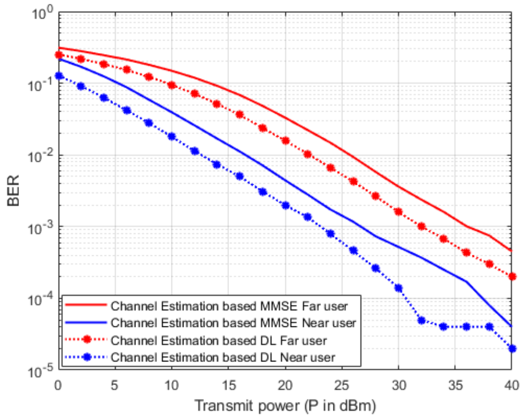

Fig. 3 BER vs Power for Ch. Est.based DL & MMSE .

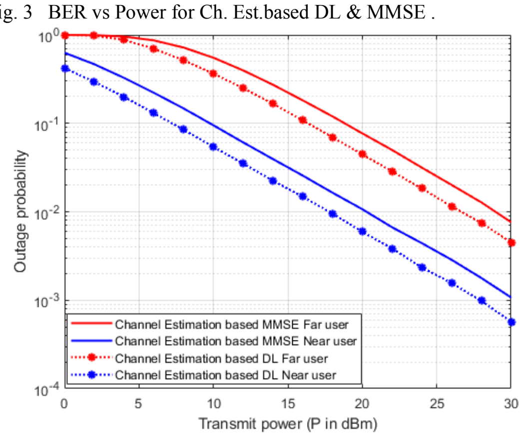

Fig. 4 Outage Prob. vs Power for Ch. Est.based DL & MMSE

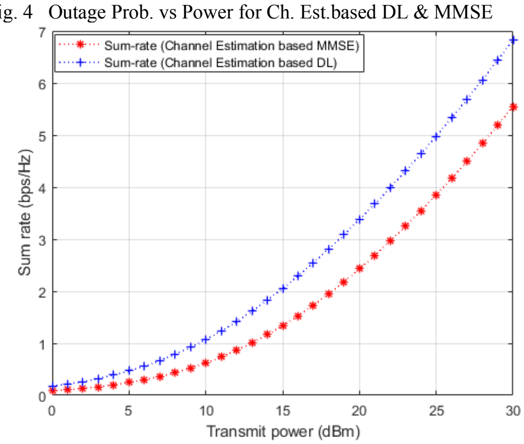

Fig. 5 Sum rate vs Power for Ch. Est.based DL & MMSE .

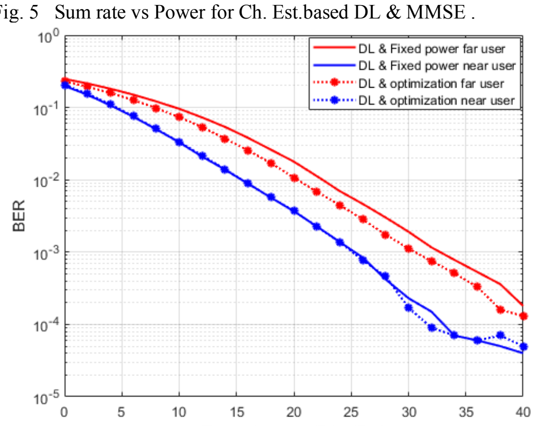

Fig. 6 BER vs Power for Ch. Est. based DL (Optimized & FPA)

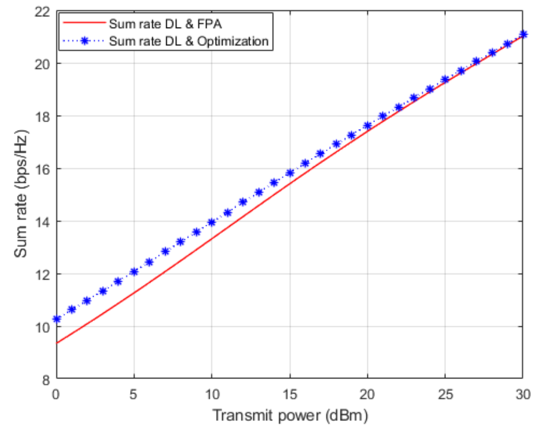

Fig. 7 Sum rate vs Power for Ch. Est. based DL (Optimized & FPA)

REFERENCES

[1] L. Dai, B. Wang, Z. Ding, Z. Wang, S. Chen, and L. Hanzo, ‘‘A survey of non-orthogonal multiple access for 5G,’’ IEEE Commun. Surveys Tuts., vol. 20, no. 3, pp. 2294–2323, 2018.

[2] M. AbdelMoniem, S. M. Gasser, M. S. El-Mahallawy, M. W. Fakhr, and A. Soliman, “Enhanced NOMA system using adaptive coding and modulation based on LSTM neural network channel estimation,” Applied Sciences, vol. 9, no. 15, 2019.

[3] A. Pourkabirian and M. H. Anisi, "Robust Channel Estimation in Multiuser Downlink 5G Systems Under Channel Uncertainties," in IEEE Transactions on Mobile Computing, 2021.

[4] Yang, Z.; Ding, Z.; Fan, P.; Karagiannidis, G.K. “On the Performance of Non-orthogonal Multiple Access Systems with Partial Channel Information”. IEEE Trans. Commun. 2016, 64, 654–667.

[5] Wang, X., Zhu, P., Li, D., Xu, Y., & You, X. “Pilot-Assisted SIMO-NOMA Signal Detection with Learnable Successive Interference Cancellation”. IEEE Communications Letters. 2021.

[6] Emir, A., Kara, F., Kaya, H., & Yanikomeroglu, H. “Deep Learning Empowered Semi-Blind Joint Detection in Cooperative NOMA”. IEEE Access, 9, 2021.

[7] J.Zhu, J. Wang, Y.Huang, S.He, X. You and L.Yang, ”On Optimal Power Allocation for Downlink Non-Orthogonal Multiple Access Systems,” in IEEE Journal on Selected Areas in Communications, vol. 35, no. 12, pp. 2744-2757, 2017.

[8] M. Gaballa, M. Abbod and A. Jameel, "Power Optimization Analysis using Throughput Maximization in MISO Non-Orthogonal Multiple Access System," 2021 IEEE Globecom Workshops, 2021.

[9] Z. Yang, W. Xu, C. Pan, Y. Pan, and M. Chen, ”On the Optimality of Power Allocation for NOMA Downlinks with Individual QoS Constraints,” IEEE Commun. Lett., vol. 21, no. 7, pp. 1649-1652, 2017.

[10] S. Boyd and L. Vandenberghe, Convex Optimization. Cambridge, U.K.: Cambridge Univ. Press, 2004.

[11] H. Ye, L. Liang, G. Y. Li, and B.-H. F. Juang, “Deep learning based end-to-end wireless communication systems with GAN as unknown channel,” IEEE Trans. Wireless Commun., vol. 19, no. 5, 2020.

[12] Gaballa, Mohamed, Maysam Abbod, and Ammar Aldallal. "Investigating the Combination of Deep Learning for Channel Estimation and Power Optimization in a Non-Orthogonal Multiple Access System." Sensors 22.10 (2022): 3666.

[13] Hochreiter, S., J. Schmidhuber, “Long short-term memory.” Neural computation. Vol. 9, Number 8, 1997.

[14] H. Ye, G. Y. Li and B. Juang, “Power of deep learning for channel estimation and signal detection in OFDM systems,” in IEEE Wireless Communications Letters, vol. 7, 2018.

[15] J. -J. van de Beek, O. Edfors, M. Sandell, S. K. Wilson and P. O. Borjesson, “On channel estimation in OFDM systems,” IEEE 45th VTC, vol. 2, pp. 815-819, Chicago, USA.

[16] Recommendation, I.R. Guidelines for Evaluation of Radio Transmission Technologies for IMT-2000 .